ENTROPY GENERATION ANALYSIS ON TWO-PHASE MICROPOLAR NANOFLUIDS FLOW IN AN INCLINED CHANNEL WITH CONVECTIVE HEAT TRANSFER

by

***Jafar HASNAIN*[a*] *and Zaheer ABBAS*[b]**

[a] Department of Computer Science, Bahria University Islamabad Campus, Islamabad, Pakistan
[b] Department of Mathematics, The Islamia University of Bahawalpur, Bahawalpur, Pakistan

Original scientific paper
https://doi.org/10.2298/TSCI170715221H

This article deals the entropy generation due to mixed convective flow of two non-miscible and electrically conducting fluids streaming through an inclined channel by considering convective boundary conditions at the walls of channel. Micropolar fluid is flowing adjacent to the upper wall of the channel and fluid flowing between the non-Newtonain fluid layer and lower plate of channel is water based nanofluid. The transformed dimensionless coupled equations are solved numerically via shooting technique. The numerical results are plotted to analyze the effects of various emerging parameters. This study shows that an increase in magnetic parameter and Brinkman number causes an increase in entropy generation whereas entropy generation reduces with increase in micropolar parameter and nanoparticle volume fraction.

Key words: *two-phase flow, micropolar fluid, nanofluid, convective boundary condition, inclined channel*

Introduction

Two-phase flow situations occur in majority of problems concerned with geophysics, plasma physics, petroleum industry, and magneto fluid dynamics. Recent literature shows certain experimental as well as analytical investigations on different aspects of two-phase flow phenomena. Shail [1] analyzed the viscous fluid-flow between a pair of horizontal insulating plates in which there was a layer of non-conducting fluid bounded by the conducting fluid and upper wall of channel. Malashetty and Umavatti [2] studied the two-phase flow enclosed by an inclined channel with heat transfer where one-phase electrically conducting. Kumar *et al.* [3] investigated the two-fluid mixed laminar flow of conducting fluid in a vertical channel with magnetic field and heat transfer. In another study, Abbas *et al.* [4] observed velocity and thermal slip effects on two-phase viscous fluid in the presence of heat transfer through an inclined channel. Recently, Hasnain *et al.* [5] presented the numerical solution on the flow of viscous and non-Newtonian (third grade) fluids through porous medium within an inclined channel.

The flow as well as heat transfer of the fluid by means of channels is of great significance because of their large range of applications in technology and engineering. These applications are established in the areas like geothermal energy removal, microfluidic devices, oil excursion, extrusion of polymer fluids, surface sublimation and binary gas diffusion. There are a

* Corresponding author, e-mail: jafar_hasnain14@yahoo.com, jafar.buic@bahria.edu.pk

variety of fluids that happens to be essential from the industrial perspective whose characteristics are not successfully described by the Navier-Stokes equations and termed as non-Newtonian fluids. In literature, various models are proposed because of the intricacy of such kinds of fluids. However, the micropolar fluid model is regarded as notable. The concept of the micropolar fluid comes from the fluid-flows consisting of rotating micro elements. In micropolar fluids, coupling among spin of each particles along with macroscopic velocity field is considered. This concept is useful to describe the flow of liquefied crystal, polymeric liquids, colloidal fluids and animal blood. Initially, Eringen [6] introduced the concept of micropolar fluids and developed new material parameters, one extra independent vector field (the microrotation) and new constitutive equations which should be solved simultaneously with the classical equations for Newtonian fluid-flow. In addition to micropolar theory sometimes called microstructure theory, Eringen [7] continued his investigation by considering heat conduction and heat dissipation effects. Fully developed flow of viscous and micropolar fluids in a channel was studied by Kumar *et al.* [8]. Sibanda and Awad [9] considered laminar flow of a micropolar fluid along a channel and found an analytical solution. By using homotopy perturbation method, Sheikholeslami *et al.* [10] studied micropolar fluid-flow through porous channel in the presence of heat transfer. Recently, Tetbirt *et al.* [11] did numerical analysis of convective heat transfer of micropolar and viscous fluid-flow in vertical channel with constant magnetic field.

The leading industrial developments of present century are affected by the nanotechnology, and consequently the researchers are attracted towards the study of nanofluids. Water, paraffin oil, ethylene glycol, kerosene and grease are some fluids which are poor conductors of heat. But thermal conductivity of such fluids has substantial impact on heat transfer phenomena. To raise the thermal conductivity of these fluids, Choi [12] proposed solid particles that are suspended in such type the fluid. The size of these particles is approximately 10-100 nm in diameter and because of their tiny size they are considerably stable as well as without additional challenges of pressure drop, sedimentation, erosion and non-Newtonian behavior. In another study, Choi *et al.*[13] noticed that the fluid's thermal conductivity increased nearly two times with the insertion of nanoparticles even though their volume is less than 1%. The heat transfer analysis of nanofluid flow through a channel with various assumptions has been carried out by several authors [14-20].

The recent development in the area of heat transfer is the investigation of entropy generation which goes back to Clausius and Kelvins who studied the irreversibility features of Second law of thermodynamics. Though, the entropy generation as a consequence of temperature difference stayed neglected by classical thermodynamics. Second law of thermodynamics includes designs of thermal devices associated with the concept of entropy generation as well as its optimization. The factors which affect the generation of entropy are viscous effects, magnetic effects and heat transfer towards lower thermal gradient *etc.* The entropy generation is involved in various energy pertinent systems like cooling of advanced electrical systems, heat exchangers, geothermal energy system, solar power collectors, energy storage systems and pipe networks. Das and Jana [21] investigated the effects of MHD flow of viscous fluid in a porous channel with entropy generation. Das *et al.* [22] discussed the entropy generation in MHD nanofluid flow in a vertical channel by considering three different types of nanoparticles. Ibanez [23] examined the effects of convective boundary condition on entropy generation of electrically conducting viscous fluid in a channel along hydrodynamic slip. Chen *et al.* [24] analyzed the entropy generation on flow of Al_2O_3-H_2O nanofluid through channel numerically. Falade *et al.* [25] considered the flow of couple stress fluid within a channel using entropy generation.

The present study aims to investigate the entropy generation analysis on mixed convective two-phase flow of an electrically conducting micropolar and nanofluid in an inclined

channel. We also considered the convective boundary conditions at the thermal heated walls. In Phase I of the channel, we considered micropolar fluid by taking a constant magnetic field, whereas Phase II is filled with water-based Ag magnetic nanoparticles. Numerical solutions of the coupled ODE are constructed using shooting method with Runge-Kutta scheme.

Formulation of the problem

Consider laminar flow of two immiscible fluids enclosed in a channel expanding *in x*- and *z*-direction. A schematic illustration of an inclined channel having inclination, ϕ, with the horizontal axis is shown in fig. 1. The domain $0 \le y \le h_1$, named as Phase I, comprises of an electrically conducting micropolar fluid and domain $-h_2 \le y \le 0$, labelled as Phase II, encloses an electrically conducting water based nanofluid. Both the fluids have densities, ρ_i, viscosities, μ_i, electrical conductivities, σ_i, thermal diffusivities, α_i, thermal conductivities, κ_i, and specific heat capacitance, C_{pi}, where $i = 1$ is for micropolar fluid, $i = s$ is for nanofluid, $i = s$ is for nanoparticles and $i = 2$ is for base fluid. The spherical particles of Ag are used as nanoparticles with φ as nanoparticle volume fraction. The fluid flow is confined to a transverse magnetic field of unvarying intensity, B_0. The fluid properties of each fluid are taken as constant and the fluid-flow in channel occurs by uniform pressure gradient ($-\partial p / \partial x$). The temperature of channel plates is preserved at uniform temperature T_{w1} and T_{w2} at $y = h_1$ and $y = -h_2$ respectively, with $T_{w1} > T_{w2}$. The fully developed flow of both fluids is steady and incompressible. Under these preliminary suppositions, the governing momentum and energy equations in the presence of magnetic field and ohmic dissipation, respectively, are presented:

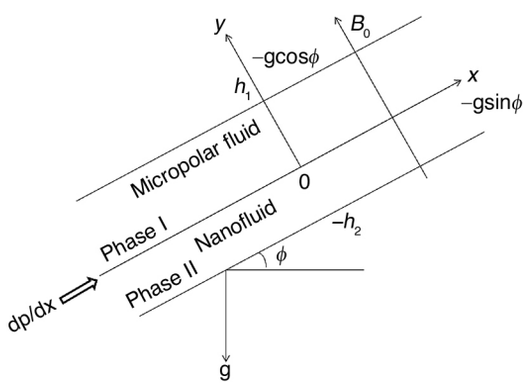

Figure 1. Physical diagram of the study

For Phase I

$$(\mu_1 + \Pi)\frac{\mathrm{d}^2 u_1}{\mathrm{d}y^2} + \Pi\frac{\mathrm{d}N}{\mathrm{d}y} + \rho_1 g\beta_1 \sin\phi\,(T_1 - T_{w2}) - \sigma_1 B_0^{\,2} u_1 = \frac{\partial p}{\partial x} \tag{1}$$

$$\gamma\frac{\mathrm{d}^2 N}{\mathrm{d}y^2} - \Pi\left(2N + \frac{\mathrm{d}u_1}{\mathrm{d}y}\right) = 0 \tag{2}$$

$$\alpha_1\frac{\mathrm{d}^2 T_1}{\mathrm{d}y^2} + \frac{\sigma_1}{\rho_1 C_{p1}} B_0^{\,2} u_1^{\,2} = 0 \tag{3}$$

$$\mu_{nf}\frac{\mathrm{d}^2 u_1}{\mathrm{d}y^2} + \rho_{nf} g\beta_{nf} \sin\phi\,(T_2 - T_{w2}) - \sigma_{nf} B_0^{\,2} u_2 = \frac{\partial p}{\partial x} \tag{4}$$

For Phase I I

$$\alpha_{nf}\frac{\mathrm{d}^2 T_2}{\mathrm{d}y^2} + \frac{\sigma_{nf}}{(\rho C_p)_{nf}} B_0^{\,2} u_2^{\,2} = 0 \tag{5}$$

where u_1 and T_i are the velocities and temperatures of the fluids, respectively, flowing in the two phases of the channel, N – the component of micro rotation vector normal to the xy – plane, γ – spin the gradient viscosity, Π – the vortex viscosity, β_1 – the coefficients of thermal expansion and g – the gravitational acceleration. For simplicity, we have neglected the viscous dissipation effects in the energy eq (3) and (5).

The expressions $\mu_{nf}, \rho_{nf}, \alpha_{nf}, \beta_{nf}, (\rho C_p)_{nf}, \sigma_{nf}$ and κ_{nf} are given as [17]:

$$\alpha_{nf} = \frac{\kappa_{nf}}{(\rho C_p)_{nf}}, \rho_{nf} = (1-\varphi)\rho_2 + \varphi\rho_s, \beta_{nf} = (1-\varphi)\beta_2 + \varphi\beta_s$$
$$\mu_{nf} = \frac{\mu_2}{(1-\varphi)^{2.5}}, \sigma_{nf} = \sigma_f\left[1 + \frac{3(\sigma-1)\varphi}{(\sigma+2)-(\sigma-1)\varphi}\right], \sigma = \frac{\sigma_s}{\sigma_f} \tag{6}$$
$$(\rho C_p)_{nf} = (1-\varphi)(\rho C_p)_2 + \varphi(\rho C_p)_s, \frac{\kappa_{nf}}{\kappa_2} = \frac{\kappa_s + 2\kappa_2 - 2\varphi(\kappa_2 - \kappa_s)}{\kappa_s + 2\kappa_2 + \varphi(\kappa_2 - \kappa_s)}$$

The thermophysical properties of water and nanoparticle are given in tab. 1.

Table 1. Thermophysical properties of water and nanoparticle

Liquid and nanoparticles	ρ [kgm^{-3}]	C_p [Jkg^{-1} K^{-1}]	κ [Wm^{-1} K^{-1}]	$\beta \cdot 10^{-5}$ [K^{-1}]	σ [Sm^{-1}]
Pure water	997.1	4179	0.613	21	$5.5 \cdot 10^{-6}$
Silver	10500	385	429	1.89	$63 \cdot 10^{6}$

The following boundary and interface conditions on velocity with continuity of shear stresses at the interface are proposed:

$$u_1(h_1) = 0 \quad u_1(0) = u_2(0), \quad u_2(-h_2) = 0 \quad N(h_1) = 0$$
$$(\mu_1 + \Pi)\frac{\mathrm{d}u_1}{\mathrm{d}y} + \Pi N = \mu_{nf}\frac{\mathrm{d}u_2}{\mathrm{d}y}, \; N = 0 \text{ at } y = 0 \tag{7}$$

and the following convective boundary and interface conditions on temperature with the continuity of heat fluxes at the interface are:

$$\kappa_1\frac{\mathrm{d}T_1}{\mathrm{d}y} + h_1^*(T_1 - T_{w2}) = 0 \text{ at } y = h_1, \; T_1(0) = T_2(0)$$
$$\kappa_{nf}\frac{\mathrm{d}T_2}{\mathrm{d}y} + h_2^*(T_2 - T_{w2}) = 0 \text{ at } y = -h_2, \; \kappa_1\frac{\mathrm{d}T_1}{\mathrm{d}y} = \kappa_{nf}\frac{\mathrm{d}T_2}{\mathrm{d}y} \text{ at } y = 0 \tag{8}$$

where h_i^* are coefficients of convective heat transfer for each plate of the channel. It is further supposed that:

$$\gamma = \left(\mu_1 + \frac{\Pi}{2}\right)j = \mu_1\left(1 + \frac{K}{2}\right)j \tag{9}$$

where j is micro-inertia density and $K = \Pi / \mu_1$ is the micropolar fluid material parameter. By taking $K = 0$ the case of Newtonian fluid can be achieved.

Using the following non-dimensional variables and parameters:

$$u_i^* = \frac{u_i}{\overline{u}_i}, y_i^* = \frac{y_i}{h_i}, N^* = \frac{h_i}{\overline{u}_i}N, \theta_i = (T_i - T_{w2})/\Delta T$$
$$m = \frac{\mu_1}{\mu_2}, k = \frac{\kappa_1}{\kappa_2}, h = \frac{h_2}{h_1}, n = \frac{\rho_2}{\rho_1}, b = \frac{\beta_2}{\beta_1}, s = \frac{\sigma_2}{\sigma_1}$$
$$\mathrm{Gr} = g\beta_1 h_1^3\frac{\Delta T}{\upsilon_1^2}, \mathrm{M} = B_0 h_1\sqrt{\frac{\sigma_1}{\mu_1}}, \mathrm{Br} = \frac{\mu_1\overline{u}_1^2}{\kappa_1\Delta T}, \xi = \frac{j}{h_1^2} \tag{10}$$
$$P = \left(\frac{h_1^2}{\mu_1\overline{u}_1}\right)\left(\frac{\partial p}{\partial x}\right), \mathrm{Re} = \frac{\overline{u}_1 h_1}{\upsilon_1}$$

where Gr, Br, Re, M, and P are the Grashof number, Brinkman number, Reynolds number, Hartmann number, and non-dimensional pressure gradient, respectively, $\overline{u}_i$, is the average velocity. The flow equations, after utilizing the previously non-dimensional quantities become:

Phase I

$$(1+K)=\frac{\mathrm{d}^2u_1}{\mathrm{d}y^2}+K\frac{\mathrm{d}N}{\mathrm{d}y}+\frac{\mathrm{Gr}}{\mathrm{Re}}\sin\phi\theta_i-\mathrm{M}^2u_1=P \tag{11}$$

$$\frac{\mathrm{d}^2N}{\mathrm{d}y^2}-\frac{2K}{2+K}\frac{1}{\xi}\left(2N+\frac{\mathrm{d}u_1}{\mathrm{d}y}\right)=0 \tag{12}$$

$$\frac{\mathrm{d}^2\theta_1}{\mathrm{d}y^2}+\mathrm{M}^2\mathrm{Br}u_1^2=0 \tag{13}$$

Phase II

$$\frac{\mathrm{d}^2u_2}{\mathrm{d}y^2}+\frac{\mathrm{Gr}}{\mathrm{Re}}bmnh^2\sin\phi\,(1-\varphi)^{2.5}\left(1-\varphi+\varphi\frac{\rho_s}{\rho_2}\right)\left(1-\varphi+\varphi\frac{\beta_s}{\beta_2}\right)\theta_2- \tag{14}$$

$$-msh^2\,\mathrm{M}^2\,(1-\varphi)^{2.5}\left[1+\frac{3(\sigma-1)\varphi}{(\sigma+2)-(\sigma-1)\varphi}\right]u_2=(1-\varphi)^{2.5}mh^2P$$

$$\frac{\kappa_{nf}}{\kappa_2}\frac{\mathrm{d}^2\theta_2}{\mathrm{d}y^2}+\mathrm{M}^2\mathrm{Br}kh^2s\left[1+\frac{3(\sigma-1)\varphi}{(\sigma+2)-(\sigma-1)\varphi}\right]u_2^2=0 \tag{15}$$

The velocity, temperature conditions (7) and (8) in non-dimensional form are:

$$\begin{gathered}u_1(1)=0,\quad u_1(0)=u_2(0),\quad u_2(-1)=0,\ N(1)=0\\(1+K)=\frac{\mathrm{d}u_1}{\mathrm{d}y}+KN=\left(\frac{1}{mh}\right)\frac{1}{(1-\varphi)^{2.5}}\frac{\mathrm{d}u_2}{\mathrm{d}y},\frac{\mathrm{d}N}{\mathrm{d}y}=0\ \text{ at }\ \mathrm{y}=0\end{gathered} \tag{16}$$

and

$$\begin{gathered}\frac{\mathrm{d}\theta_1}{\mathrm{d}y}+\mathrm{Bi}_1\theta_1=0\ \text{at}\ y=1,\ \theta_1(0)=\theta_2(0)\\\frac{\mathrm{d}\theta_2}{\mathrm{d}y}-\frac{\kappa_2}{\kappa_{nf}}\,\mathrm{Bi}_2\theta_2=0\ \text{at}\ y=-1,\frac{\mathrm{d}\theta_1}{\mathrm{d}y}=\frac{1}{kh}\frac{\kappa_{nf}}{\kappa_2}\frac{\mathrm{d}\theta_2}{\mathrm{d}y}\ \text{at}\ \ y=0\end{gathered} \tag{17}$$

where $\mathrm{Bi}_1 = h_1 h_1^*/\kappa_1$ and $\mathrm{Bi}_2 = h_2 h_2^*/\kappa_2$ are Biot numbers for upper and lower plates, respectively. Usually the Biot number is taken same for both plates.

Entropy generation

Entropy generation occurs due to non-equilibrium conditions which appear by virtue of energy exchange, magnetic field as well as momentum within the fluid and at the walls of the channel. In the absence of viscous dissipation, heat transfer and magnetic effects are the components of entropy generation. The volumetric rate of entropy generation for incompressible micropolar fluid is given:

$$S_{G1}=\frac{\kappa_1}{T_{w2}^2}\left(\frac{\mathrm{d}T_1}{\mathrm{d}y}\right)^2+\frac{\sigma_1B_0^2}{T_{\mathrm{w}2}}u_1^2 \tag{18}$$

and the volumetric rate of entropy generation for incompressible nanofluid is given as:

$$S_{G2}=\frac{\kappa_{nf}}{T_{w2}^2}\left(\frac{\mathrm{d}T_2}{\mathrm{d}y}\right)^2+\frac{\sigma_{nf}B_0^2}{T_{\mathrm{w}2}}u_2^2 \tag{19}$$

The dimensionless form of eqs. (18) and (19) are expressed:

$$Ns_1=\left(\frac{\mathrm{d}\theta_1}{\mathrm{d}y}\right)^2+\frac{\mathrm{Br}}{T_p}\mathrm{M}^2u_1^2 \tag{20}$$

and

$$Ns_2=\frac{1}{kh^2}\frac{\kappa_{nf}}{\kappa_2}\left(\frac{\mathrm{d}\theta_2}{\mathrm{d}y}\right)^2+\frac{\mathrm{Br}}{T_p}\left[1+\frac{3(\sigma-1)\varphi}{(\sigma+2)-(\sigma-1)\varphi}\right]\mathrm{M}^2su_2^2 \tag{21}$$

where Ns_i is the dimensionless entropy generation number and $T_p=\Delta T/T_{w2}$ is the dimensionless temperature difference. Combining eqs. (20) and (21) give the overall entropy generation number Ns throughout the channel and is expressed:

$$Ns = Ns_1 + Ns_2$$
$$Ns = \left(\frac{\mathrm{d}\theta_1}{\mathrm{d}y}\right)^2 + \frac{1}{kh^2}\frac{\kappa_{nf}}{\kappa_2}\left(\frac{\mathrm{d}\theta_2}{\mathrm{d}y}\right)^2 + \frac{\mathrm{Br}}{T_p}\,\mathrm{M}^2 u_1^{\,2} + \frac{\mathrm{Br}}{T_p}\left[1 + \frac{3\,(\sigma-1)\,\varphi}{(\sigma+2)-(\sigma-1)\,\varphi}\right]\mathrm{M}^2 s u_2^{\,2} \tag{22}$$

The first two terms on R.H.S. of eq. (23) represent entropy generation caused by heat transfer and the last two terms express the entropy generation due to magnetic field.

With a purpose to analyze the dominance of heat transfer irreversibility on irreversibility due to magnetic field and vice versa, Bejan number is defined [22]:

$$\mathrm{Be} = \frac{\text{entropy generation due to the heat transfer}}{\text{entropy generation number}}$$

The heat transfer irreversibility dominates when Be > 0.5 and magnetic field irreversibility is dominant when Be < 0.5.

Results and discussion

Numerical solution of eqs. (11)-(15) subject to the boundary conditions (16) and (17) is obtained using shooting method to exhibit the physical understanding of the flow problem under the influence of various flow parameters. The algorithm of the numerical scheme is given in fig. 2. Figures 3-6 demonstrate the impact of six parameters on the linear fluid velocity, angular fluid velocity, and temperature of fluid, the parameters are: micropolar parameter, K, magnetic parameter, M, ratio of heights, h, ratio of electrical conductivities, s, nanoparticle volume fraction φ, and Biot numbers Bi_1, Bi_2. Figures 7-10 and tabs. 2 and 3 are presented to show the influence of micropolar parameter, K, magnetic parameter, M, nanoparticle volume fraction, φ, inclination angle, ϕ, dimensionless pressure gradient, P, and Brinkman number on entropy generation and Bejan number.

Figures 3 shows the influence of micropolar parameter, K, and magnetic parameter, M, on linear fluid velocity $u(y)$, microrotation/angular fluid velocity $N(y)$ as well as fluid temperature $\theta(y)$ keeping other parameters fixed. Figures 3(a) shows the effects on linear fluid velocity $u(y)$ due to change in micropolar parameter, K, with two values of magnetic parameter, M. The increase in micropolar parameter, K, as well as magnetic parameter, M, causes decrement in linear fluid velocity $u(y)$ in the channel. But this decrease in the velocity of fluid in Phase I is more prominent instead of Phase II, since it contains micropolar fluid. On the other side, the decrease in fluid velocity with the increasing value of magnetic parameter, M, is because of the retarding force, named as Lorentz force, which increases with an increase in magnetic parameter. Since both the fluids are electrically conducting so fluid velocity

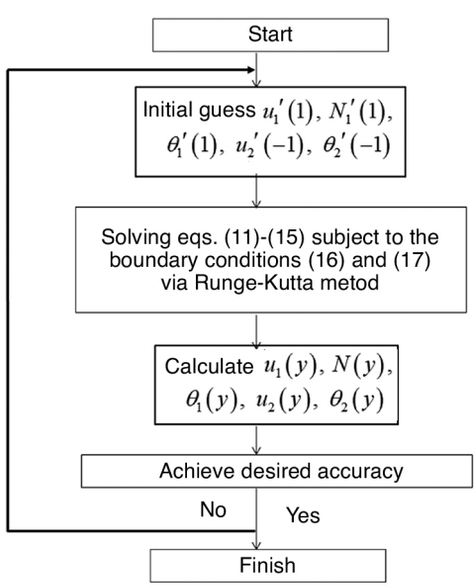

Figure 2. Flow chart of the numerical method.

throughout the channel is decreased with an increment in the magnetic parameter but when micropolar parameter isincreased a significant change is observed in velocity of the fluid in the Phase I whereas change in the fluid velocity in Phase II is the result of continuity. The curves plotted in fig. 3(b) show the change in the microroation velocity $N(y)$ with increase in micropolar parameter and magnetic parameter. The magnitude of microrotation velocity $N(y)$ increases with a hike in micropolar parameter whereas an inflation in magnetic parameter, as expected, causes a decline in the microrotation velocity. The variation in fluid temperature $\theta(y)$ with the rise in both micropolar parameter and magnetic parameter can be seen in fig. 3(c). From this figure, it can be observed that an increase in magnetic parameter provokes an increase in temperature of fluid $\theta(y)$ whereas reverse behavior is observed with an increase in micropolar parameter.

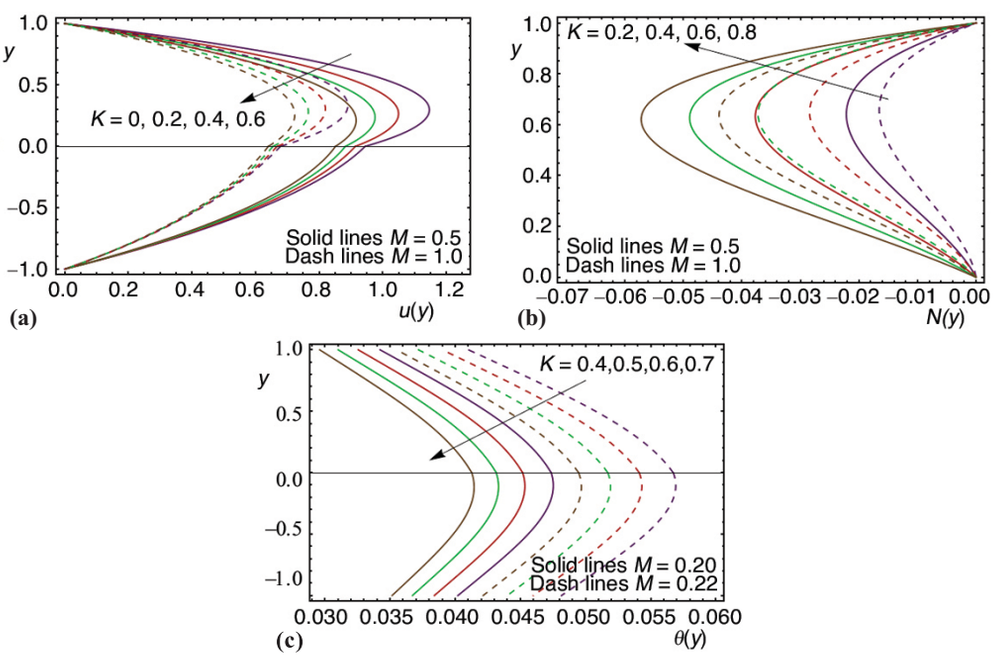

Figure 3. (a) Velocity distribution, (b) microrotation velocity distribution, (c) temperature distribution for several values of micropolar parameter and magnetic parameter

Figures 4 displays the change in linear velocity of fluid, angular fluid velocity and fluid temperature for several values of ratio of heights, h, as well as ratio of electric conductivities s of fluids. Figure 4(a) shows the influence of ratio of heights and ratio of electric conductivities on linear fluid velocity $u(y)$. One can observe from the figure that fluid velocity increases with an increase in height of upper phase relative to the lower phase. It can also be observed that flow field is much larger in the upper phase of channel as compared to lower phase but this difference is decreased with an increase ratio of heights. The decreasing behavior of linear velocity with an increase in ratio of electric conductivities is also noticed in this figure. The variation in angular fluid velocity $N(y)$ is exhibited in fig. 4(b). It can be seen clearly from the figure that the angular velocity $N(y)$ is decreased as the ratio of heights, h, increases, whereas it is increased by the increasing values of s. The effect of ratio of heights, h, and ratio of electric conductivities, s, on fluid temperature $\theta(y)$ is shown fig. 4(c). This figure depicts that as both ratio of heights and ratio of electric conductivities increases, an increase in temperature of fluid $\theta(y)$ is witnessed. Also, the

temperature field in the lower phase is smaller when compared to the upper phase of the channel. The effects of change in ratio of electrical conductivities on temperature field is much prominent at greater values of ratio of heights.

The impact of nanoparticle volume fraction, φ, on the fluid velocity $u(y)$ and fluid temperature $\theta(y)$ is plotted in fig. 5. An increase in nanoparticle volume fraction, φ, results in the decrement of both fluid velocity $u(y)$ and temperature of fluid $\theta(y)$ as can be noticed in figs. 5(a) and 5(b), respectively. From both figures, it is also noticed that if non-Newtonian fluid (micropolar fluid) in the upper phase of channel is swapped by a Newtonain fluid (viscous fluid), the influence of nanoparticle volume fraction, φ, continues to be same. Yet the magnitude of velocity and temperature profiles for viscous nanofluids system is larger rather than micropolar nano fluids system. The curves plotted in fig. 6 show the effect of Biot numbers on temperature of fluid $\theta(u)$ by considering both Newtonian ($K = 0$) and non-Newtonian fluids ($K = 0.2$). The limit $Bi_1 \to 0$ and $Bi_2 \to 0$ means that both the walls of channel are thermally isolated and no heat transfer occurs whereas $Bi_1 \to \infty$ and $Bi_2 \to \infty$ correlate to the situation when each ambient temperature and that of fluid at the wall are equal. Furthermore, the heat flow from the walls of channel to ambient temperature increases as Biot number increases which leads to the decrement in temperature of fluid.

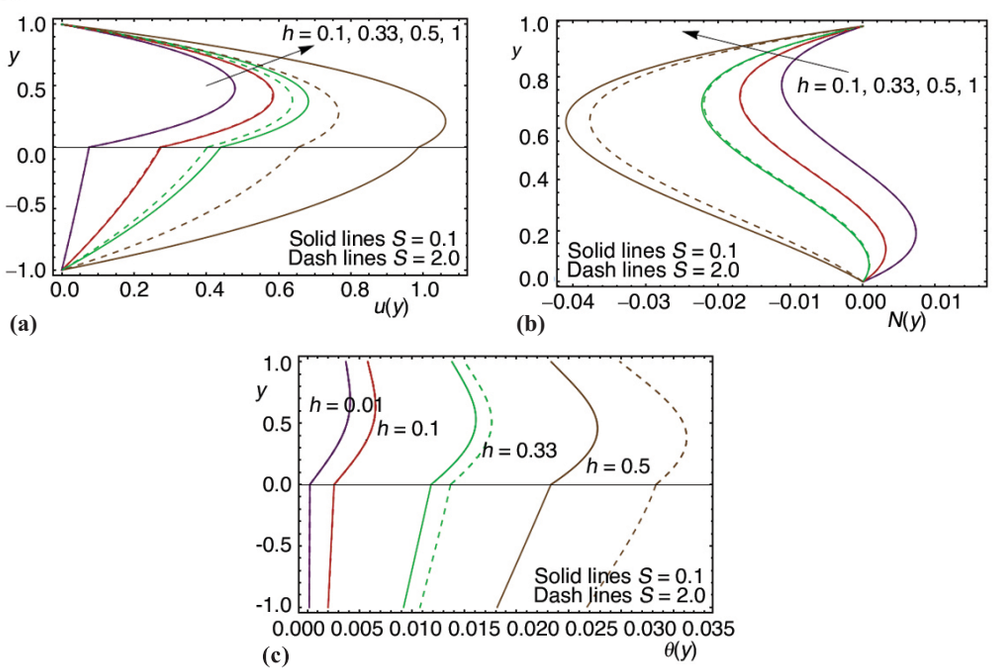

Figure 4. (a) Velocity distribution, (b) microrotation velocity distribution, (c) temperature distribution for several values of ratio of heights h and ratio of electrical conductivities

Figure 7 is displayed to present the effects of micropolar parameter, *K,* on the entropy generation number, *Ns,* and Bejan number. From the figure it is clear that both entropy generation number and Bejan number decrease with the increasing values of microploar parameter. An increase in entropy generation number, *Ns,* and decrease in Bejan number is observed with hike in magnetic parameter, *M*. Figure 8 demonstrates this phenomena, whereas the variation in entropy generation within the channel for micropolar fluid is lesser than nanofluid see fig. 8(a). Figure 9

elucidates the changing behavior of entropy generation number, *Ns,* and Bejan number as nanoparticle volume fraction, φ, varies. The decreasing nature of entropy generation number and increasing behavior of Bejan number is seen in this figure. The variation in entropy generation number, *Ns,* and Bejan number with the increasing values of Brinkman number is depicted in fig. 10. This figure reveals that with the increase of Brinkman number the rate of entropy generation increases, conversely, the decrement in Bejan number is noted. Physically, Brinkman number represents heat generation source therefore in the layers of moving fluid, heat is generated. Hence entropy generation is increased in the channel due to this heat generation along with heat transfer at the walls.

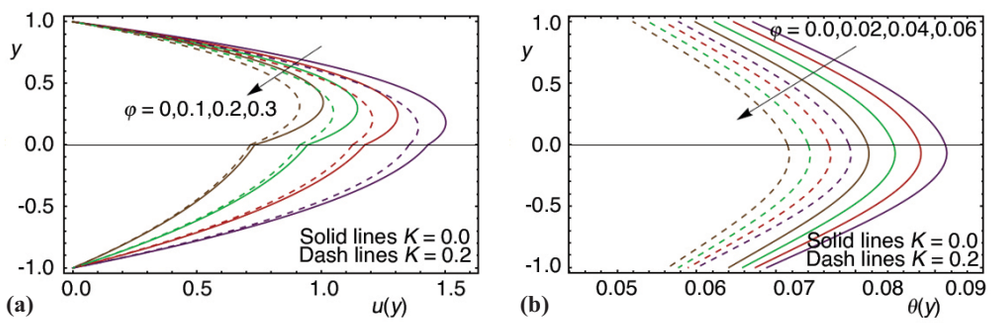

Figure 5. (a) Velocity distribution, (b) temperature distribution for several values of nanoparticle volume fraction and micropolar parameter

Tables 2 presents the change in fluid velocity as well as fluid temperature with in the channel with an increase in the inclination of the channel. It can be noticed from the table that an increase in the inclination angle leads to decrease velocity along with the temperature of the fluid. The effect of dimensionless pressure gradient on velocity and temperature profiles is presented in table 3. One can observe that a hike in both fluid velocity and temperature is produced with the increasing values of *P*. The tables also show that the flow field for the micropolar fluid in larger than that of nanofluid.

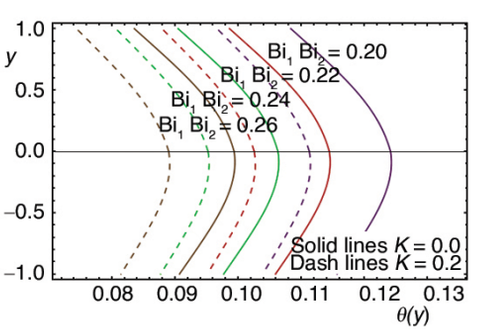

Figure 6. Temperature distribution for several values of Biot number and micropolar parameter.

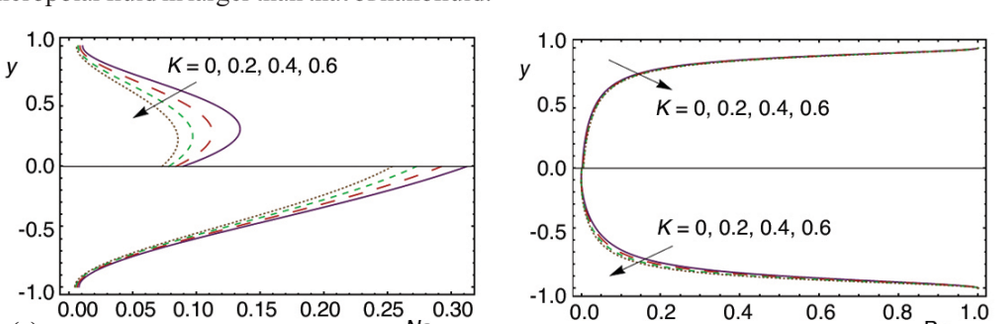

Figure 7. (a) Entropy generation (b) Bejan number for several values of micropolar parameter

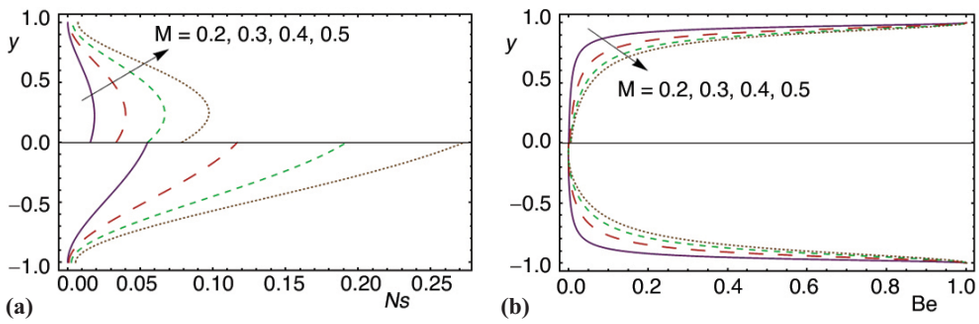

Figure 8. (a) Entropy generation (b) Bejan number for several values of magnetic parameter

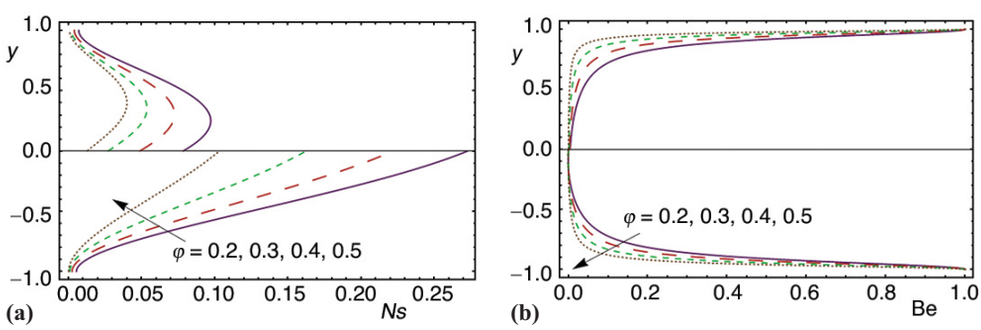

Figure 9. (a) Entropy generation (b) Bejan number for several values of nanoparticle volume fraction

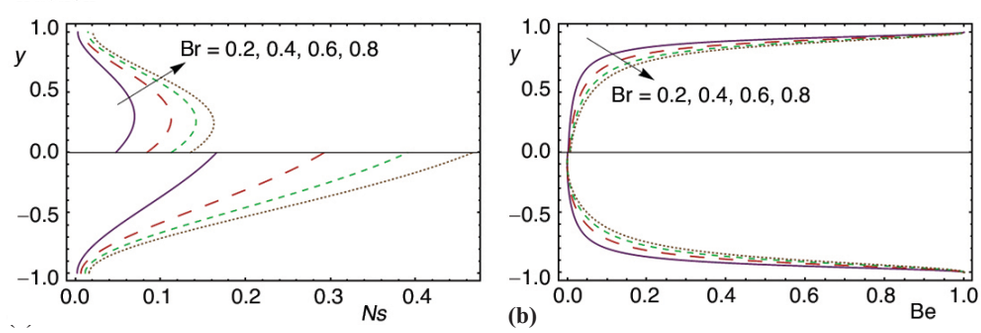

Figure 10. (a) Entropy generation (b) Bejan number for several values of Brinkman number

Concluding remarks

In this study, an entropy generation analysis is performed due to mixed convection and magnetic field in an inclined channel for the flow of two non-miscible fluids with convective boundary conditions. The two fluids taken in the study are non-Newtonian (micropolar) fluid and Newtonian base-nanofluid. The numerical solutions of the transformed ODE are found by shooting technique. The outcomes of the study can be sum up as follows.

- The linear velocity of fluid $u(y)$ leads to decline with hike in K, M, s, and φ whereas increase in h of channel increases the fluid velocity.
- Magnitude of microrotation fluid velocity $N(y)$ increases by increasing the values of K, h while opposite trend is noticed with increase in M and s.
- Decrease in fluid temperature $\theta(y)$ with in the channel is examined with rise in K and φ and Biot numbers, however increase in M, h, and s enhances the fluid temperature.

- Increase in entropy generation occurs due to increase in M and Br but escalating values of K and φ decrease the entropy generation.
- Bejan number decreases with an increase in φ while contrary behavior is noted for Br, K and M.

Table 2. Velocity and temperature for different values of inclination of channel

y	$\phi = 0$		$\phi = \pi / 6$		$\phi = \pi / 4$	
	u	θ	u	θ	u	θ
1.00	0.00000	0.034950	0.00000	0.034240	0.00000	0.033957
0.80	0.460880	0.038431	0.446171	0.037650	0.440873	0.037339
0.60	0.789350	0.041751	0.762141	0.040902	0.752345	0.040563
0.40	0.979162	0.044640	0.942088	0.043729	0.928744	0.043365
0.20	1.028090	0.046869	0.984064	0.045905	0.968223	0.045520
0.00	0.937058	0.048359	0.889119	0.047357	0.871878	0.046956
−0.20	0.850399	0.048401	0.803393	0.047393	0.786490	0.046990
−0.40	0.714974	0.047378	0.673291	0.046388	0.658305	0.045993
−0.60	0.529426	0.045598	0.497406	0.044644	0.485895	0.044263
−0.80	0.291895	0.043398	0.273796	0.04248	0.267290	0.042126
−1.00	0.000000	0.041057	0.00000	0.040197	0.00000	0.039854

Table 3. Velocity and temperature for different values of dimensionless pressure gradient

y	$\rho = 2$		$\rho = 4$		$\rho = 6$	
	u	θ	u	θ	u	θ
1.00	0.00000	0.005545	0.00000	0.022002	0.00000	0.049108
0.80	0.181851	0.006098	0.359103	0.024194	0.532275	0.053999
0.60	0.311113	0.006625	0.613720	0.026284	0.908782	0.058663
0.40	0.385359	0.007083	0.759129	0.028101	1.122620	0.062715
0.20	0.403748	0.007436	0.793733	0.029500	1.171520	0.065835
0.00	0.366668	0.007672	0.718351	0.030434	1.056760	0.067914
−0.20	0.332162	0.007678	0.649631	0.030457	0.954084	0.067964
−0.40	0.278897	0.007516	0.544766	0.029812	0.799094	0.066523
−0.60	0.206322	0.007233	0.402636	0.028627	0.590085	0.064021
−0.80	0.113678	0.006884	0.221700	0.027306	0.324711	0.060930
−1.00	0.000000	0.006513	0.00000	0.025834	0.00000	0.057644

Nomenclature

B_0 − magnetic fiend, [T]
b − ratio of coefficient of thermal expansion of phases, [$= \beta_2/\beta_1$], [−]
Bi_i − biot number, [$= h_i h_i^*/\kappa_i$]
Be − bejan number [−]
Br − brinkman number [$= \mu_1 u_1^{-2}/\kappa_1 \Delta T$]
C_p − specific heat at constant pressure, [$\mathrm{Jkg^{-1}K^{-1}}$]
Gr − grashof number, [$= g\,\beta_1\,h_1^3\,(T_{w1}-T_{w2})/v_1^2$]
g − acceleration due to gravity, [$\mathrm{LT^{-2}}$]
h_i − heights of the phases, [L]
h − ratio of heights of phases, [$= h_2/h_1$], [−]
K − micropolar parameter, [$= \Pi/\mu_1$]
k − ratio of coefficient of thermal conductivity of fluids of phases, [$= K_1/K_2$] [−]
k^* − mean absorption coefficient
M − hartman number [$= B_0 h_2 \sqrt{\sigma/\mu_2}$]
m − ratio of coefficient of dynamic viscosity of phases [$= \mu_1/\mu_2$] [−]
N − micro-rotation vector [−]
n − ratio of densities of fluids of phases [$= \rho_1/\rho_1$], [−]
− nondimensional pressure gradient, [−]
P − reynolds number, [−]
Re − ratio of electrical conductivities of
s fluids of phases [$= \sigma_2/\sigma_1$], [−]

T_i – temperature of the fluid of phases, [K]
T_{wi} – temperature at the surfaces ot the plates of the phases
u_i – velocity of phases x-direction, [ms^{-1}]
u_i^* – dimensionless velocities of phases, [ms^{-1}]
u_1 – average velocity, [ms^{-1}]
x,y,z – spatial co-ordinates [m]
y_i^* – dimensional variable

Greek symbols

α_i – thermal diffusivities of the phases, [m^{2}s^{-1}]
β_i – coefficient of thermal expansion, [K^{-1}]
γ – spin gradient viscosity
μ_i – dinamic viscosities of the phases, [–]
κ_i – thermal conductivity of fluidsof phases, [Wm^{-1}K^{-1}]
υ_i – kinematic viscosities of the phases, [m^{2}s^{-1}]
Π – vortex viscosity
ρ_i – fluid densities of the phases, [kgm^{-3}]
θi – dimensionless temperatures of the phases, [$=(T - T_{w2})/(T_{w1} - T_{w2})$] [–]
ϕ – angle of the channel with horizontal, [rad]
σ_i – eletrical conductivities of fluid, [sm^{-1}]
φ – ratio of coefficient of dynamic viscosity of phases [$= \mu_1/\mu_2$] [–]

Subscripts

w – surface conditions
i – for phase I $i = 1$, for phase II $i = 2$, for nanofluids $i = nf$, for nanoparticles $i = s$

Acknowledgment

We are thankful to the anonymous reviewer for his/her useful comments to improve the version of the paper.

References

[1] Shail, R. On Laminar Two-Phase Flows in Magnetohydrodynamics, *Int. J. Engng. Sci.,11* (1973), 10, pp. 1103-l 108
[2] Malashetty, M. S., Umavathi, J. C., Two-Phase Magnetohydrodynamic Flow and Heat Transfer in an Inclined Channel, *Int. J. Multiphase Flow, 23* (1997), 3, pp. 545-560
[3] Kumar, J. P., *et al.*, Two-fluid Mixed Magnetoconvection Flow in a Vertical Enclosure*, J. Appl. Fluid Mech., 5* (2012), 3, pp. 11-21
[4] Abbas, Z., *et al*., MHD Two-Phase Fluid Flow and Heat Transfer with Partial Slip in an Inclined Channel, *Thermal Science*, *20,* (2016), 5, pp.1435-1446
[5] Hasnain, J., *et al*., Effects of Porosity and Mixed Convection on MHD Two Phase Fluid Flow in an Inclined Channel, *Plos One*, *10* (2015), 3, e0119913
[6] Eringen, A. C., Theory of Micropolar Fluids, *J. Math. Mech.,16* (1966), 1, pp. 1-18
[7] Eringen, A. C., Theory of Thermomicropolar Fluids, *J. Math. Anal. Appl., 38* (1972), 2, pp. 480-496
[8] Kumar, J. P., *et al*., Fully-Developed Free-Convective Flow of Micropolar and Viscous Fluids in a Vertical Channel, *Appl. Math. Model, 34* (2010), 5, pp. 1175-1186
[9] Sibanda, P., Awad, F. G., Flow of a Micropolar Fluid in Channel with Heat and Mass Transfer, *Proceedings*, Inte. Cont. on Theoretical and Applied Mechanics, and Inte. Cont. on Fluid Mechanics and Heat and Mass Transfer, Corfu Island, Greece, 2010, pp. 112-120
[10] Sheikholeslami*,* M., *et al*., Micropolar Fluid Flow and Heat Transfer in a Permeable Channel Using Analytical Method, *J. Molec. Liq., 194* (2014), June, pp. 30-36
[11] Tetbirt, A., *et al.*, Numerical Study of Magnetic Effect on the Velocity Distribution Field in a Macro/Micro – Scale of a Micropolar and Viscous Fluid in a Vertical Channel, *J. Molec. Liq., 216* (2016), Apr., pp. 103-110
[12] Choi, S.U.S., Enhancing Thermal Conductivity of Fluids with Nanoparticles, *Proceedings,* ASME International Mechanical Engineering Congress and Exposition, San Francisco, Cal. USA,1995,Vol 66, pp. 99-105
[13] Choi, S.U.S., *et al*., Anomalously Thermal Conductivity Enhancement in Nanotube Suspensions, *Appl. Phys. Lett., 79* (2001), 14, pp. 2252-2254
[14] Oztop, H. F. Abu-Nada, E., Numerical Study of Natural Convection in Partially Heated Rectangular Enclosures Filled with Nanofluids, *Int. J. Heat Fluid Flow, 29* (2008), 5, pp. 1326-1336
[15] Sheikholeslami, M., *et al*., Analytical Investigation of MHD Nanofluid Flow in a Semi-Porous Channel, *Powder Technology, 246* (2013), Sept, pp. 327-336
[16] Fersadou, I., *et al*., MHD Mixed Convection and Entropy Generation of a Nanofluid in a Vertical Porous Channel, *Computers & Fluids, 121* (2015), Oct, pp. 164-179
[17] Das, S., *et al*., Mixed Convection Magnetohydrodynamic Flow in a Vertical Channel Filled with Nanofluids, *Eng. Sci. Tech., Int. J., 18* (2015), 2, pp. 244-255
[18] Abolbashari, M. H., *et al*., Analytical Modeling of Entropy Generation for Casson Nano-Fluid Flow Induced by a Stretching Surface, *Advanced Powder Technology, 26* (2015), 2, pp. 542-552

[19] Khalili, S., *et al*., Unsteady Convective Heat and Mass Transfer in Pseudoplastic Nanofluid Over a Stretching Wall, *Advanced Powder Technology, 26* (2015), 5, pp. 1319-1326
[20] Bhatti, M. M., Rashidi, M. M., Effects of Thermo-Diffusion and Thermal Radiation on Williamson Nanofluid over a Porous Shrinking/Stretching Sheet, *J. Molec. Liq. 221* (2016), Sept., pp. 567-573
[21] Das, S., Jana, R. N., Entropy Generation Due to MHD Flow in a Porous Channel with Navier Slip, *Ain Shams Eng. J., 5* (2014), 2, pp. 575-584
[22] Das, S., *et al*., Entropy Analysis on MHD Pseudo-Plastic Nanofluid Flow Through a Vertical Porous Channel with Convective Heating, *Alexandria Eng. J., 54* (2015), 3, pp. 325-337
[23] Ibanez, G., Entropy Generation in MHD Porous Channel with Hydrodynamic Slip and Convective Boundary Conditions, *Int. J. Heat Mass Trans., 80* (2015), Jan., pp. 274-280
[24] Chen, C.-K., *et al*., Entropy Generation in Mixed Convection Magnetohydrodynamic Nanofluid Flow in Vertical Channel, *Int. J. Heat Mass Trans., 91* (2015), Dec., pp. 1026-1033
[25] Falade, J. A., *et al*., Entropy Generation Analysis for Variable Viscous Couple Stress Fluid Flow Through a Channel with Non-Uniform Wall Temperature, *Alexandria Eng. J., 55* (2016), 1, pp, 69-75

Paper submitted: July 15, 2017
Paper revised: October 4, 2017
Paper accepted: October 10, 2017